Nuclear Physics B159 (1979) 56–66

NEUTRON-NUCLEUS INELASTIC CROSS SECTIONS FROM 160 TO 375 GeV/c *

T.J. ROBERTS, H.R. GUSTAFSON, L.W. JONES, M.J. LONGO and M.R. WHALLEY

Department of Physics, University of Michigan, Ann Arbor, Michigan 48109, USA

Received 3 April 1979
(Final version received 6 July 1979)

We have measured inelastic cross sections of neutrons on 14 nuclei ranging from hydrogen to uranium for neutron energies between 160 and 375 GeV. The measurements were made with a total absorption calorimeter and have an accuracy of 1%. The results are compared to other data and predictions of the Glauber model. Interaction lengths for high-energy neutrons in composite materials of practical interest are also given.

1. Introduction

We have measured the inelastic cross sections of neutrons on various nuclei over the energy range from 50 to 400 GeV. The measurements were made at Fermi National Laboratory with a neutron beam produced by 400 GeV protons incident on a beryllium target **. The physics interest in the inelastic cross sections arises from the effects which the rising nucleon-nucleon total cross sections and the energy-dependent inelastic screening have on the Glauber-model calculation. In earlier measurements of total cross sections it was established that it was necessary to include the inelastic screening term to bring the data into agreement with the Glauber calculation [2]. The inelastic cross section is also of considerable practical interest, as it and not the total cross section is relevant to the interaction length of neutrons in matter. This in turn relates to important questions in the choice of targets, shielding and cosmic ray air shower development, for example.

Little published data on hadron inelastic cross sections at high energy is extant, in spite of the wide use of such numbers. There are two older experiments from below 100 GeV [3,4] and a recent experiment with charged hadrons at Fermilab [5]. The neutron-nucleus inelastic cross sections at high energies should be very nearly equal to those for incident protons. However, we believe that the neutron experiment is simpler and more straightforward than the corresponding proton

* Work supported by US National Science Foundation.
** Preliminary reports of this experiment were presented in ref. [1].

experiment because Coulomb effects are insignificant and most inelastic interactions can be simply identified by the emergence of one or more charged particles from the target. In comparing different experiments it is important to keep in mind that systematic differences might occur because of different treatment of "quasielastic" interactions, i.e., those interactions in which the incident particle scatters on a nucleon in the target nucleus so that nuclear excitation and/or nucleon emission occurs, but not meson production.

It is important to clearly identify the components of the total cross section σ_T:

$$\sigma_T = \sigma_E + \sigma_Q + \sigma_I \,, \tag{1}$$

Here σ_E is the coherent elastic scattering, σ_Q is the "quasielastic" scattering, i.e., scattering wherein the nucleus is disrupted but there are no mesons produced, and σ_I is the inelastic interaction leading to meson production. Of interest also is the "absorption" cross section σ_A defined as

$$\sigma_A \equiv \sigma_Q + \sigma_I \,. \tag{2}$$

2. Experimental method

The experiment is a straightforward poor-geometry transmission measurement (fig. 1). The neutron beam was collimated to a diameter of approximately 4 mm at the target. A 7.5 cm Pb filter followed by sweeping magnets approximately 100 m from the production target effectively removed γ's and charged particles. The neutron beam was transported over most of its 500 m path in vacuum. Targets were mounted so that they could be placed into or out of the beam on alternate beam pulses. Interacting neutrons were identified by a pulse from a scintillation counter B, 10 X 10 cm^2, which was placed approximately 8 cm beyond the target midplane. The beam

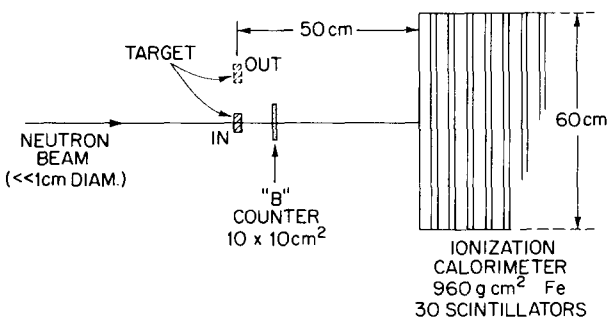

Fig. 1. The experimental arrangement. (Note that transverse dimensions have *not* been exaggerated.)

Table 1
Neutron-nucleus inelastic cross sections (mb)

	Energy (GeV) (bin center)						
Nucleus	182	222	262	302	348	$\bar{\sigma}$(160-375)	Mean free path λ (g/cm^2)
H[a)]	32.9	32.5	33.7	33.5	32.5	32.9	50.9
D[a)]						61.5	54.3
Be	198	199	200	199	201	199	75.0
C	236	237	237	240	240	237	84.0
Al	428	425	429	434	433	430	103
Fe	715	714	721	723	726	721	129
Cu	789	791	793	798	799	794	133
Zn	805	807	820	817	822	814	133
Cd	1188	1182	1196	1203	1204	1196	156
Ta	1648	1643	1651	1665	1673	1646	181
W	1684	1687	1693	1695	1696	1691	180
Pb	1785	1786	1811	1816	1822	1808	190
U	1978	1986	2025	2047	2069	2024	195
H_2O						353	84.7
D_2O						410	81.0
Air[b)]						270	90.3

Quasielastic scattering not included.
Errors are ±1%, due mostly to systematic uncertainty in unobserved target nucleon diffraction dissociation and to details of target measurements, except hydrogen (±1.5%). Corrections of +1% (heavy elements) to +2% (light elements) have been added to the experimental data to correct for the unobserved final states of target nucleon diffraction dissociation.

a) Cross sections derived from compounds: CH_2, H_2O, D_2O, and C. Systematic errors on these are ±1.5%.

b) Air derived assuming 68%N, 21%O, 1%Ar; σ for N and Ar derived from neighboring measurements.

neutrons and/or secondaries produced in the target were detected by a total absorption calorimeter [6] of area 60 × 60 cm^2, located 50 cm beyond the target, which provided a measure of the energy of the incident neutron. Since essentially all of the secondaries were collected in the calorimeter, the energy measurement was nearly independent of whether or not the incident neutron interacted. The incident neutron spectrum was continuous with an approximately triangular shape, peaking near 320 GeV and extending from 0 to 400 GeV. Pulses from the calorimeter were binned according to pulse height by means of discriminators, which divided the spectrum into 7 energy bins. Data from the lowest two energy bins are not reported, however, because of uncertainties in the K° contamination of the beam. The centers of the energy bins are noted in table 1. The discriminator with the lowest threshold was used to measure the total neutron flux (20-400 GeV).

The uncorrected cross sections were calculated for each target in each pulse-height (energy) interval from the ratio of the fraction of neutrons transmitted with target in to that with target out,

$$\sigma_i = -(nx)^{-1} \ln[(C_i\bar{B}/C_0)_{\text{in}}/(C_i\bar{B}/C_0)_{\text{out}}] , \tag{3}$$

where nx is the number of target nuclei per cm^2, C_0 is the total number of counts in the calorimeter and $C_i\bar{B}$ is the number of events in a particular pulse-height bin for which the B counter saw no charged particles. As a consequence of the observed energy independence of the cross sections, it was found useful to calculate $\bar{\sigma}$, the cross section averaged over incident neutrons with energies between 160 and 375 GeV.

3. Systematic errors and checks

Several sources of possible systematic error were identified and studied. These are discussed below.

3.1. Interactions which do not register in the B counter

Some fraction of the interactions may not register in the B counter because: (a) only secondaries of insufficient range to penetrate a thick target are produced; (b) the solid angle subtended by B (about 1 sr) is too small; (c) reactions in which only π^0's are produced may escape detection if π^0's are not converted in the target.

To study effects (a) and (c), cross sections were measured with various thicknesses of U, W, C, and Be targets to find evidence for a dependence of σ on target thickness. No evidence for such a dependence for targets up through 35% of a mean free path (U) was detected. The thinnest targets also gave the same cross sections within statistics, down to $\sim$1 g $\cdot$ cm^{-2} of Be. Most data were taken with a target thickness corresponding to about 0.1 interaction mean free path. Data were also taken with 1.5 rad lengths of lead and with 5 g $\cdot$ cm^{-2} of carbon between the target and B. Again no changes in cross sections were seen at the 1% level. To study effect (b), the size of the B counter was varied as well as its spacing from the target. For the normal B-target spacing we estimate 0.5% error due to interactions from which all charged secondaries are outside the solid angle subtended by B. A correction for this has been applied to all quoted results.

Events in which a target nucleon undergoes diffraction dissociation to an N* with N$^* \rightarrow$ N + π's would often not count in the B counter. Gaisser et al. [7] have estimated that

$$\sigma(\text{n} + \text{N} \rightarrow \text{n} + \text{N}^*) \cong \frac{\sigma_{\text{D}}(\text{NN})}{\sigma_{\text{I}}(\text{NN})} [\tfrac{2}{3}\pi\langle R\rangle^2] , \tag{4}$$

where σ_{D}(NN) is the single diffraction dissociation cross section for the target proton

in the nucleon-nucleon interaction, $\sigma_I(NN)$ is the corresponding inelastic cross section and $\langle R \rangle$ is the r.m.s. nuclear radius. From data of Chapman et al. [8], Albrow et al., [9] and others, $\sigma_D(NN) \simeq 3.5$ mb at 400 GeV, so that $\sigma_D/\sigma_I \simeq 0.1$. When typical values of $\langle R \rangle$ are used, $\sigma(n + N \to n + N^*)$ amounts to from 6% (Be) to 3% (U) of the measured nuclear inelastic cross section. About half of the N^* production may result in two-body final states, $N\pi$, while half may result in three (or more) body states [8]. From the geometry of the apparatus, about 40% of the $N\pi$ final states should be detected, so that the correction to the cross sections varies from 2% (Be) to 1% (U). The detection efficiency for $N\pi\pi$ and $N\pi\pi\pi$ final states is much higher, and no correction was made for those processes.

Beam particle diffraction dissociation such as $n + A \to (n + \pi^\circ) + A$ can also pass undetected, if none of the γ's convert in the target. For multiple π° production, our detection efficiency is high enough, and the cross section is low enough that no correction is required. Single π° production should be $\frac{1}{2}$ of the process $n + A \to (p\pi^-) + A$, which has a cross section of 0.67% (Be) to 1.25% (Pb) of the inelastic total [10]. The π° detection probability ranges from ~0.3 (Be) to ~0.9 (Pb), so the correction is 0.4% (Be) to 0.1% (Pb).

Quasielastic interactions, wherein a target nucleon is ejected from the nucleus without meson production, are *not* detected in this experiment. An attempt was made to detect this process by reducing the Be target thickness to 1 $g \cdot cm^{-2}$, but no increase in cross section could be detected. Nucleons ejected from the nucleus would be half neutrons which would not be detected in counter B in any case. Only a small fraction of the protons could count in the B counter which only subtended about 10% of the lab solid angle. A more severe constraint is the proton range; a proton must have >25 MeV (K.E.) to penetrate 1 $g \cdot cm^{-2}$ of Cu while most nuclear evaporation protons would have a K.E. of <20 MeV. Direct recoils from np elastic scattering are peaked at 50 MeV, corresponding to a range of 3 $g \cdot cm^{-2}$ (Cu). In addition, a negligible fraction of prompt nuclear β and γ decays would be detected in the B counter. Therefore any fraction of the quasielastic cross section σ_Q detected would appear to be well below 5%. As the σ_Q is calculated to be <10% of σ_I, we estimate that quasi-elastic events contribute $\ll 0.5\%$ of the measured cross sections *.

3.2. Kaon and gamma contamination of the beam

The kaon contamination in the beam was estimated by studying the effect of enriching the fraction of K°'s by placing thick carbon attenuators in the beam, as described in ref. [2]. The kaon contamination was ~15-20% below 95 GeV, ~4-6% between 95 and 160 GeV and $\lesssim$ 2% in the energy bin from 160 to 204 GeV. Above 200 GeV the kaon fraction is negligible. A correction was made to the cross sec-

* We are indebted to G. Yodh and T. Gaisser for extensive discussion of the diffraction and quasielastic correction questions.

tions in the 160-204 GeV bin ($\bar{E} \simeq 182$ GeV) and the two lower bins; however the kaon fraction varied with neutron beam production angle and it was not possible to make a satisfactory, simple correction in the two lowest energy bins. Consequently results are reported here only for energies above 160 GeV.

The lead in the beam was varied from 1.2 cm to 7.5 cm and effects on σ and the shape of the calorimeter spectrum were studied to look for evidence of γ contamination. No difference was seen between 5 and 7.5 cm of Pb and data were taken always with 7.5 cm in the beam.

3.3. Backscattering from the calorimeter

Backscatter from the calorimeter causes counts in the B counter for a small fraction ($\lesssim \frac{1}{2}\%$) of the incident neutrons *. There is also a very small contamination of charged particles in the beam ($\ll 1\%$). Neither of these effects produce an error in cross sections as they cancel in the target in/out ratio.

3.4. Beam intensity and rate effects

Possible dependence of the measured cross sections on beam intensity was studied by varying the incident intensity over a wide range. The data used in the analysis were from intensities about ten times lower than those where there was any evidence for rate effects. Accidental rates were also recorded and served as a sensitive monitor of rate fluctuations. Abnormal beam spills were deleted.

3.5. Energy mismeasurement causing bin-edge crossing

Bin-edge crossing due to the calorimeter resolution cancels in the target in/out ratio, so it is not a problem. Neutrons which interact in the target may leave an appreciable fraction of their energy in the target (mainly due to the electromagnetic cascade in thick, heavy targets) or may have secondaries which miss the calorimeter. This causes serious difficulties when calculations are performed using the number of neutrons interacting in the target. As we calculate cross sections from the number of neutrons which do *not* interact in the target, these problems do not affect our results.

* From measurements of $C \cdot B/C$ as a function of the separation between counter B and the calorimeter, it was found that charged-particle backscatter (albedo) from the calorimeter was 8% at 8 cm from the face of the calorimeter and fell almost as the solid angle subtended from a point about 8 cm into the calorimeter.

4. Results

The measured cross sections, corrected as described above, are recorded in table 1 Also tabulated is $\bar{\sigma}$, the average cross section over the energy interval 160-375 GeV. When $\bar{\sigma}$ is fitted to a power law in A, a good fit for $A \geqslant 9$ is found of the form

$$\sigma_I(\mathrm{nA}) = \sigma_0 A^{\alpha} \tag{5}$$

with $\sigma_0 = 41.2$ mb and $\alpha = 0.711$. The fit is shown in fig. 2, which also shows n-nucleus total cross-section data previously measured by our group [2] and the corresponding power-law fit.

Each cross section represents a statistical average over thousands of individual cross-section measurements, which in turn represent one beam spill with target in and the adjacent (preceding or succeeding) beam spill with target out. Occasional anomalous spills (with bad spill structure, etc.) were rejected. The distributions of measured cross section correspond to standard deviations of less than $\frac{1}{4}\%$, except for CH_2 and H_2O ($<\frac{1}{2}\%$). Other sources of error include systematic uncertainties in target thickness, (or nx) in eq. (3) of $\pm\sim\frac{1}{2}\%$, and uncertainties in the corrections for undetected cross sections as discussed above ($\sim\frac{1}{2}\%$).

Our best estimate of the uncertainty in each cross section is 1%, mostly due to

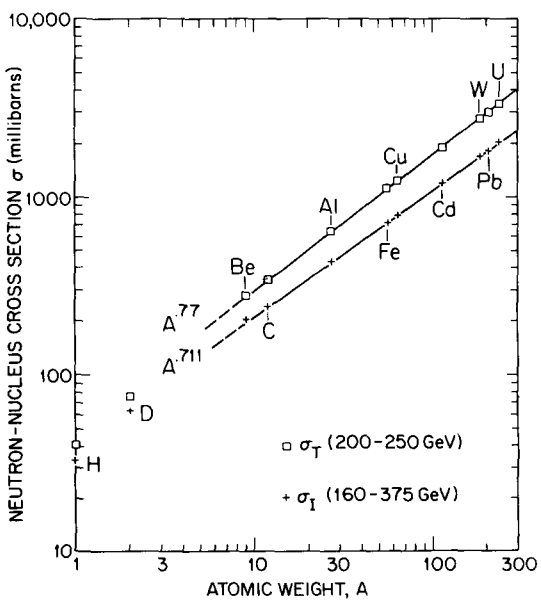

Fig. 2. Inelastic cross sections (160 to 375 GeV) *versus* atomic weight compared with the lower-law fit. Neutron-nucleus total cross sections from ref. [2] are also shown (upper curve and data points).

the systematic uncertainties. The errors on hydrogen, deuterium and oxygen are somewhat larger as a result of their determination from differences: CH_2–C (hydrogen), H_2O–H_2 (oxygen), and D_2O–H_2O (deuterium).

5. Discussion

In measurements of proton-nucleus inelastic cross sections at 20 GeV/c^2, Bellettini et al., observed a discrete quasielastic cross-section component in the light elements ($6 \leqslant A \leqslant 27$) which they assumed also applied to the heavy elements [3]. They assumed that

$$\sigma_Q \simeq 13A^{1/3} \text{ mb} . \tag{6}$$

Gaisser et al. [7] arrived at a different expression based on a Glauber calculation:

$$\sigma_Q = 0.19(2.3\pi\langle R\rangle^2) \simeq 3.8A^{2/3} \text{ mb} . \tag{7}$$

The two expressions agree for $A \simeq 40$ and are within a few mb for lighter nuclei; however they disagree by 66 mb for U^{238}, or about 3% of σ_I.

The cross sections which are most easily compared with a Glauber model are σ_T and σ_E. However in many practical applications such as the calculation of hadron attenuation in material or hadron punch-through, the cross section of interest is σ_I. In another context, particle production in complex nuclei is often parametrized in terms of ν, the average number of interactions of a nucleon in a nucleus, given by

$$\nu = A\sigma_I(\text{NN})/\sigma_I(\text{NA}) .$$

In this case σ_I *without* σ_Q is the appropriate cross section to use, not $\sigma_A \equiv \sigma_I + \sigma_Q$ as measured in ref. [3] and used in papers on this subject [11]. It is unclear from ref. [4] whether the values therein are σ_A or σ_I; the difference between them varies from 10% (C) to 7% (U) (eq. (7)).

Comparing our inelastic cross sections with the proton-nucleus measurements of ref. [5], for the same energies, we find that our cross sections individually are generally in good agreement with theirs, which have quoted errors (systematic) ≈3%. However, an overall comparison shows our results are systematically higher with the difference ranging from ≈5% for carbon to ≈2% for lead. Their cross sections have been corrected for quasielastic scattering (using the Bellettini et al., [3] expression, eq. (6)) and so should be directly comparable to ours. The reason for the discrepancy is unknown. However, their technique requires an extrapolation to "t" = 0, which involves a correction to their data ~10% for carbon; the t range for the partial cross sections used in the extrapolation and the fitting function chosen are somewhat arbitrary. Our corrections to the raw data were only 1 to 2%.

It is of interest to study table 1 for evidence of change in cross sections with energy. For most elements there is a systematic rise in σ from 182 to 348 GeV of 1–1.5%. For any one element this effect would be on the edge of statistical signifi-

Table 2
Comparison of calculated and measured total and inelastic cross sections

E (GeV)	σ_T[a] (calc)	σ_T (meas)[b]	σ_A	σ_Q	σ_I (calc)	σ_I (meas) (this exp)
Beryllium: $\langle R\rangle$ = 2.556 fm, $R_{1/2}$ = 2.14 fm						
182	269.7	271.1	224	26[c]	198	198
222	271.6	273.5	224		198	199
262	271.6	270.8	225		199	200
302	272.7	273.8	226		200	199
348	274.1		227		201	201
Carbon: $\langle R\rangle$ = 2.536 fm, $R_{1/2}$ = 2.10 fm						
182	332	331	264	26[c]	238	236
222	333	334	265		239	237
262	334	332	266		240	237
302	335	328	267		241	240
348	337		268		242	240
Aluminium: $\langle R\rangle$ = 3.072 fm, $R_{1/2}$ = 3.07 fm						
182	634	635	469	38[c]	431	428
222	635	633	470		432	425
262	637	634	471		433	429
302	639	629	473		435	434
348	642		475		437	433
Copper: $\langle R\rangle$ = 3.891 fm, $R_{1/2}$ = 4.35 fm						
182	1229	1223	841	60[c]	781	789
222	1232	1238	843		783	791
262	1234	1231	844		784	793
302	1237	1225	846		786	798
348	1241		849		789	799
Lead: $\langle R\rangle$ = 5.528 fm, $R_{1/2}$ = 6.68 fm						
182	2946	2951	1820	122 (78)	1698 (1742[d])	1785
222	2947	2959	1821		1699 (1743[d])	1786
262	2948	2926	1823		1701 (1745[d])	1811
302	2952	2919	1824		1702 (1746[d])	1816
348	2957		1829		1707 (1751[d])	1822

[a] All values are in mb.
[b] Measurements from ref. [2]. Energy bins are: 180, 215, 240 and 273 GeV.
[c] $\sigma_Q = 0.19\ (\frac{2}{3}\pi\langle R\rangle^2)$ mb, from ref. [7]. Values in parentheses are $\sigma_Q = 13\,A^{1/3}$ mb, from ref. [3].
[d] Values of σ_I in parentheses using σ_Q from ref. [3].

cance. however for all of the pure element targets a similar rise is seen (0.7–2.0% for 10 of the 11). Only hydrogen shows no rise, but these cross sections have the largest error (±1.5%).

Table 3
Interaction lengths for neutrons between 160 and 375 GeV

	g/cm^2
Plastic scintillator	81.4
Earth (topsoil)	88.7
Concrete (ordinary)	99.8
Glass	97.8
Wood (maple)	84.4
Lucite	80.7

Elastic and quasielastic scattering not included.

The Glauber screening model, modified to include effects of inelastic screening as described in ref. [2], was used to calculate total and elastic scattering cross sections from which inelastic cross sections could be obtained. Table 2 presents the calculated and measured total and inelastic cross sections. Total cross sections were calculated as in ref. [2] using a Woods-Saxon potential with a skin thickness of 2.3 fm and values of half-density radii $R_{1/2}$ and corresponding r.m.s. radii $\langle R\rangle$ as noted on the table. Values of $R_{1/2}$ and $\langle R\rangle$ were adjusted slightly from those in ref. [2] to give values of σ_T in agreement with experiment for energies about 150 GeV. The energies selected for calculation correspond to the bin center values for the present experiment; somewhat different values were used for the ref. [2] data as noted in the footnotes. Cross sections σ_A were calculated by subtracting coherent elastic scattering as calculated from Glauber theory from σ_T, with modifications for inelastic screening as prescribed by Gaisser et al. [7]. Specifically, the correction to σ_A for inelastic screening, $\Delta\sigma_A$, is calculated using $\Delta\sigma_A(A) \simeq \frac{1}{4}\Delta\sigma(2A)$, where $\Delta\sigma_T(2A)$ is the inelastic screening correction to the total cross section for a nucleus of twice the atomic number. The quasielastic scattering, σ_Q, calculated according to ref. [7], is tabulated and subtracted from σ_A to compare with the measured cross section $\sigma_I = \sigma_A - \sigma_Q$. For lead, where the two values of σ_Q differ markedly, σ_Q from ref. [3] is also tabulated with corresponding values of σ_I. Very reasonable agreement is observed between the data and the calculations except for lead. Other heavy elements, W and U, show the same discrepancy.

It may be concluded that the nuclear interaction cross sections of nucleons at high energies are in good agreement with standard theory modified for inelastic screening, with the exception of the heaviest elements. A slight rise in inelastic cross section is detectable between 180 and 350 GeV.

Collision lengths for inelastic scattering, not including quasielastic scattering, for materials of practical interest such as concrete, iron, earth, etc., are tabulated in table 3.

It is a pleasure to acknowledge the cooperation and assistance of the staff of the Meson Laboratory in implementing this experiment. We also wish to thank J. Prentis who assisted with the Glauber calculations.

References

[1] L.W. Jones, H.R. Gustafson, M.J. Longo, T. Roberts, and M. Whalley, 15th Int. Cosmic Ray Conf., Plovdiv, 1977, to be published;
T. Roberts et al., Bull. Am. Phys. Soc. 23 (1978) 635.
[2] P.V. Ramana Murthy et al., Nucl. Phys. B92 (1975) 269.
[3] G. Bellettini et al., Nucl. Phys. 79 (1966) 609.
[4] S.P. Denisov et al., Nucl. Phys. B61 (1973) 62.
[5] A.S. Carroll et al., Phys. Lett. 80B (1979) 319.
[6] L.W. Jones et al., Nucl. Instr. 118 (1974) 431.
[7] T.K. Gaisser, G.B. Yodh, V. Barger and F. Halzen, 14th Int. Cosmic Ray Conf., Munich, Proc. 7 (1975) 2161.
[8] J.W. Chapman et al., Phys. Rev. Lett. 32 (1974) 257.
[9] M.G. Albrow et al., Nucl. Phys. B108 (1976) 1.
[10] W. Mollet et al., Phys. Rev. Lett. 39 (1977) 1646.
[11] J.E. Elias et al., Phys. Rev. Lett. 41 (1978) 285;
W. Busza et al., Phys. Rev. Lett. 34 (1975) 836.